Proceedings of the Seventh IASTED International Conference
POWER AND ENERGY SYSTEMS
August 29–31, 2007, Palma de Mallorca, Spain
ISBN Hardcopy: 978-0-88986-689-8 / CD: 978-0-88986-690-4

ROBUST MAXIMUM POWER POINT TRACKING METHOD FOR PHOTOVOLTAIC CELLS

Chen-Chi Chu and Chieh-Li Chen*
Department of Aeronautics and Astronautics,
National Cheng Kung University.
Tainan, Taiwan
*Email addresses: chiehli@mail.ncku.edu.tw

ABSTRACT
Due to nonlinear I-V characteristics of Photovoltaic (PV) cells, an MPPT algorithm is adopted to maximize the output power. In this paper, an approach for peak power tracking using the sliding mode control is proposed. The proposed controller is robust to environment changes and load variations. The stability and robustness of the controller are addressed. The performance of the controller is verified through simulations and experiments. It demonstrated that the proposed approach can be implemented effectively and economically.

KEY WORDS
Photovoltaic, Maximum Power Point Tracking, Sliding Mode, Stability.

1. Introduction

Rising oil price and more restricted environmental regulations increase the demand of utilizing alternative power sources. Hence it becomes an important topic and attracts many researchers to join in this field. Solar energy seems to be a prime candidate because it is pollution free and provides constant energy income. Among solar energy applications, PV has been paid much attention because it seems to be the most feasible application in the near future. However, the difficulties to promote PV system are the high cost and low conversion efficiency. Furthermore, the performance of PV depends on solar insolation, ambient temperature, and load impedance. Letting PV has maximum peak power (MPP) output is essential for PV applications.

The issue of tracking the MPP has been addressed in many literatures by proposing different algorithms. Among these algorithms, Hill-Climbing [1]-[3] and Perturbation-and-observation (P&O) [4]-[5] are commonly used due to their easy and cheap implementation. These two methods share the same principle by perturbing duty cycle (or PV voltage) and observing the power output. The drawback of the methods is that, at steady state, operation point (OP) oscillates around MPP, which makes the OP impossible to match with the MPP. Hence the Increment Conductance (IncCond) [6]-[8] is developed to overcome this defect. The idea of IncCond is based on the fact that the MPP is defined by the PV power (P_{PV}) to the PV voltage (V_{PV}) slope. If $dP_{PV}/dV_{PV} = 0$ is satisfied, then the MPP is perfectly tracked. When $dP_{PV}/dV_{PV} > 0$ (or $dP_{PV}/dV_{PV} < 0$), then the OP is on the left (or right) of the MPP, and should be tuned toward opposite direction. The expression of dP_{PV}/dV_{PV} can be replaced by measurable parameters $dI_{PV} / dV_{PV} + I_{PV} / V_{PV}$ where V_{PV} and I_{PV} are PV voltage and PV current, respectively. However, both P&O (or Hill-Climbing) and IncCond are badly performed during rapid changing of atmospheric conditions. Modified methods or other MPPT techniques [11]-[13] have also been proposed featuring advantages to improve tracking performance.

The algorithms mentioned above are sharing the same idea of "searching for MPP". Since PV exhibits nonlinear I-V characteristics, solutions of MPP are hardly to be determined analytically. Another approach called proportional open-circuit voltage (or short-circuit current) is addressed in [9][14]. By assuming voltage (V_{mpp}) or current (I_{mpp}) of MPP is proportion to PV open-circuit voltage (V_{oc}) or short-circuit current (I_{sc}). For example, the reasonable proportional constant of V_{mpp} to V_{oc} ranges from 0.71 to 0.78. The estimated V_{mpp} can be easily determined by sensing V_{oc}. However, the estimated V_{mpp} is only an approximation of true V_{mpp} and also note that the proportional constant will change if PV module ages, causes the performance degraded with time. But these methods require less computation, which can reduce the implementation complexity.

Typically, MPPT consists of two major components PV modules and DC-DC converters. The purpose of DC-DC converter is to control the solar module having maximum power output. By deliberately defining the sliding surface equal to the definition of MPP, we conclude that this approach is feasible to track the MPP. The proposed control strategy is robust to variation of load and atmospherical condition; it is also easy to be implemented on digital systems. Also note that, this method is relatively faster than other MPP approaches. The MPP can be achieved in tens of milliseconds.

The paper is organized as follows: In section 2, PV characteristic is described. The system model of the proposed sliding control approach MPPT is discussed in section 3. The sliding approach is given in section 4. Simulation results are given in section 5.

2. PV Characteristics

PV array is a p-n junction semiconductor, which converts light into electricity. When the incoming solar energy exceeds the band-gap energy of the module, photons are absorbed by materials to generate electricity. The equivalent-circuit model of PV is shown in Fig. 1. In this model, it consists of a light-generated source, diode, series and parallel resistances. The mathematical expression of the equivalent model can be written as (1), (2) and (3). Where R_s is relatively small and R_{sh} is relatively large, which are neglected in the equation in order to simplify the simulation.

$$I = I_{ph} - I_d\left[\exp\left(\frac{q}{k_b TA}V\right) - 1\right] \quad (1)$$

$$I_{ph} = S\left[I_{scr} + k_i\left(T - T_r\right)\right] \quad (2)$$

$$I_d = I_{rr}\left[\frac{T}{T_r}\right]^3 \exp\left(\frac{qE_g}{kQA}\left[\frac{1}{T_r} - \frac{1}{T}\right]\right) \quad (3)$$

where

I, V	output current, voltage (A, V)
T	cell temperature (K)
S	solar irradiance (W/m^2)
I_{ph}	light-generated current
I_d	PV saturation current
I_{rr}	saturation current at T_r
I_{scr}	short circuit current at reference condition
T_r	reference temperature
K_i	short circuit temperature coefficient
q	charge of an electron
k_b	Boltzmann's constant
E_g	band-gap energy of the material
Q	total electron charge
A	ideality factor

The PV characteristic is plotted in Fig. 2 under different irradiance levels, and PV characteristic under different temperature is plotted in Fig. 3. As illustrated in the figures, open circuit voltage (V_{oc}) is dominated by temperature, and solar irradiance has preeminent influence on short circuit current (I_{sc}). We can conclude that high temperature and low solar irradiance will reduce the power conversion capability.

3. MPPT System Modelling

Consider a boost type converter connected to a PV module with a resistive load as illustrated in Fig. 4.

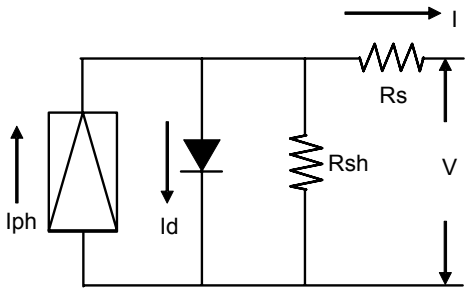

Fig. 1 Equivalent circuit model of PV

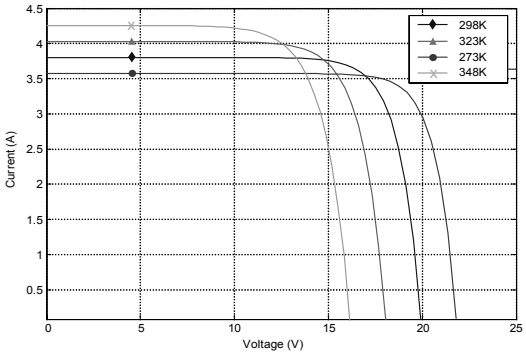

Fig. 2 PV characteristic under different temperature (Constant irradiance = 1000W/m^2)

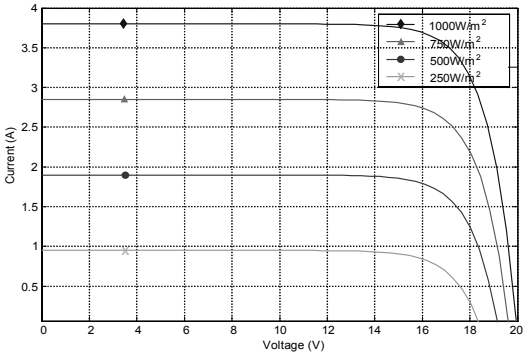

Fig. 3 PV characteristic under different irradiance levels (Constant temperature = 273K)

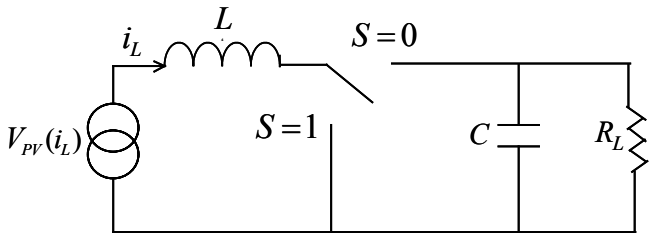

Fig. 4 MPPT system schematic

The system can be written in two sets of state equation depends on the position of switch S. If the switch is in position 0, the differential equation can be written as:

$$\dot{i}_{L_1} = \frac{V_{PV}(i_L)}{L} - \frac{V_o}{L} \quad (4a)$$

$$\dot{V}_{o_1} = \frac{i_L}{C} - \frac{V_o}{CR_L} \tag{4b}$$

The differential equation can be expressed as (5a) and (5b) if the switch is in position 1.

$$\dot{i}_{L_2} = \frac{V_{PV}(i_L)}{L} \tag{5a}$$

$$\dot{V}_{o_2} = -\frac{V_o}{CR_L} \tag{5b}$$

By utilizing State Space Averaging method [16], equation (4) and (5) can be combined into one set of state equation to represent the dynamic of the system. Base on the idea of Pulse-Width Modulation (PWM), the ratio of the switch in position 1 in a period is defined as duty ratio. Two distinct equation sets are weighted by the duty ratio and superimposed:

$$\dot{\mathbf{X}} = (1-\delta)\dot{\mathbf{X}}_1 + \delta\dot{\mathbf{X}}_2 \tag{6}$$

where $\dot{\mathbf{X}}_1 = [\,\dot{i}_{L_1} \quad \dot{V}_{o_1}\,]^{\mathrm{T}}$, $\dot{\mathbf{X}}_2 = [\,\dot{i}_{L_2} \quad \dot{V}_{o_2}\,]^{\mathrm{T}}$, and $\delta \in [0 \quad 1]$ is the duty ratio. Hence the dynamic equation of the system can be derived from equation (4)-(6):

$$\dot{i}_L = \frac{V_{PV}(i_L)}{L} - \frac{V_o}{L} + \frac{V_o}{L}\delta \tag{7a}$$

$$\dot{V}_o = \frac{i_L}{C} - \frac{V_o}{CR_L} - \frac{i_L}{C}\delta \tag{7b}$$

where C is the capacity, L is the inductance, R_L is the resistive load, $\delta \in [0 \quad 1]$ is the duty ratio, which is also the control input. V_o is the output voltage and i_L is the inductor current. Note the equivalent series resistance (ESR) of the inductor and wiring resistance are neglected in the case, so i_L is assumed to be equal to the PV current (I) in equation (4). Equation (7) can be written in general form.

$$\dot{\mathbf{X}} = f(\mathbf{X}) + g(\mathbf{X})\delta \tag{8}$$

A nonlinear time invariant system is obtained. Further nonlinear control techniques are required.

4. Approach for MPPT

A typical sliding mode control has two modes of operation. One is called the approaching mode, where the system state converges to a pre-defined manifold named sliding function in finite time. The other mode is called the sliding mode, where the system state is confined on the sliding surface and is driven to the origin. In this study, we introduce the concept of the approaching control approach. By selecting the sliding surface as $dP_{PV}/dI_{PV} = 0$, it is guaranteed that the system state will hit the surface and produce maximum power output persistently.

$$\frac{\partial P_{PV}}{\partial I_{PV}} = \frac{\partial I_{PV}^2 R_{PV}}{\partial I_{PV}} = I_{PV}(2R_{PV} + I_{PV}\frac{\partial R_{PV}}{\partial I_{PV}}) = 0 \tag{9}$$

where $R_{PV} = V_{PV} / I_{PV}$ is the equivalent load connect to the PV, and I_{PV} is the PV current, which is equal to i_L in this case. The non-trivial solution of (9) is $2R_{PV} + I_{PV} \cdot \partial R_{PV} / \partial I_{PV} = 0$. Hence, the sliding surface is defined as:

$$\sigma \triangleq 2R_{PV} + i_L \frac{\partial R_{PV}}{\partial i_L} \tag{10}$$

Based on the observation of duty cycle versus operation region as depicted in Fig. 5, the duty cycle output control can be chosen as:

$$\delta_{\text{update}} = \begin{cases} \delta + \Delta\delta & \text{for} \quad \sigma > 0 \\ \delta - \Delta\delta & \text{for} \quad \sigma < 0 \end{cases} \tag{11}$$

In order to get the equivalent control (δ_{eq}) suggested by Filippov [15], the equivalent control is determined from the following condition:

$$\dot{\sigma} = \left[\frac{\partial \sigma}{\partial \mathbf{X}}\right]^T \dot{\mathbf{X}} = \left[\frac{\partial \sigma}{\partial \mathbf{X}}\right]^T (f(\mathbf{X}) + g(\mathbf{X})\delta_{eq}) = 0 \tag{12}$$

The equivalent control is then derived:

$$\delta_{eq} = -\frac{\left[\frac{\partial \sigma}{\partial \mathbf{X}}\right]^T f(\mathbf{X})}{\left[\frac{\partial \sigma}{\partial \mathbf{X}}\right]^T g(\mathbf{X})} = 1 - \frac{V_{PV}(i_L)}{V_o} \tag{13}$$

since the range of duty cycle must lies in $0 \le \delta_{eq} \le 1$, the real control signal is proposed as:

$$\delta = \begin{cases} 1 & \delta_{eq} + k\sigma \ge 1 \\ \delta_{eq} + k\sigma, & \text{for} \quad 0 < \delta_{eq} + k\sigma < 1 \\ 0 & \delta_{eq} + k\sigma \le 0 \end{cases} \tag{14}$$

where the control saturate if $\delta_{eq} + k\sigma$ is out of range, and k is a positive scaling constant. The proposed control is comprised with δ_{eq} and $k\sigma$, where δ_{eq} is the required effort for $\dot{\sigma} = 0$ and $k\sigma$ can be considered as the effort to track the MPP. The existence of the approaching mode of the proposed sliding function σ is provided.

A Lyapunov function is defined as:

$$V \triangleq \frac{1}{2}\sigma^2 \tag{15}$$

The time derivative of σ can be written as:

$$\dot{\sigma} = \left[\frac{\partial \sigma}{\partial X}\right]^T \dot{X}$$

$$= (3\frac{\partial R_{PV}}{\partial i_L} + i_L \frac{\partial^2 R_{PV}}{\partial {i_L}^2})(-\frac{V_o}{L}(1-\delta) + \frac{V_{PV}(i_L)}{L}) \tag{16}$$

Replacing R_{PV} by the definition of $R_{PV} = V_{PV} / I_{PV}$

$$\frac{\partial R_{PV}}{\partial i_L} = \frac{\partial}{\partial i_L}\left[\frac{V_{PV}}{i_L}\right] = \frac{1}{i_L}\frac{\partial V_{PV}}{\partial i_L} - \frac{V_{PV}}{{i_L}^2} \tag{17}$$

$$\frac{\partial^2 R_{PV}}{\partial {i_L}^2} = \frac{1}{i_L}\frac{\partial^2 V_{PV}}{\partial {i_L}^2} - \frac{2}{{i_L}^2}\frac{\partial V_{PV}}{\partial i_L} + \frac{2V_{PV}}{{i_L}^3} \tag{18}$$

By (1), the PV voltage (V_{PV}) can be rewritten as function of PV current (I_{PV})

$$V_{PV} = \frac{K_b TA}{q} \ln\left(\frac{I_{ph} + I_d - I_{PV}}{I_d}\right) \quad (19)$$

$$\frac{\partial V_{PV}}{\partial I_{PV}} = -\frac{K_b TA}{q} \frac{I_0}{I_{ph} + I_0 - I_{PV}} < 0 \quad (20)$$

$$\frac{\partial^2 V_{PV}}{\partial {I_{PV}}^2} = -\frac{K_b TA}{q} \frac{I_0}{(I_{ph} + I_0 - I_{PV})^2} < 0 \quad (21)$$

Substitute (13) and (14) into (12) yield

$$\left[\frac{\partial \sigma}{\partial \mathbf{X}}\right]^T = 3\frac{\partial R_{PV}}{\partial i_L} + i_L \frac{\partial^2 R_{PV}}{\partial {i_L}^2}$$
$$= \frac{1}{i_L}\frac{\partial V_{PV}}{\partial i_L} - \frac{V_{PV}}{{i_L}^2} + \frac{\partial^2 V_{PV}}{\partial {i_L}^2} < 0 \quad (22)$$

according to the result of (20) and (21) and $V_{PV} / {i_L}^2 > 0$, the sign of (22) is negative definite.

The achievability of $\sigma = 0$ will be obtained by $\sigma\dot{\sigma} < 0$ for all δ discussed as follows.

For $0 < \delta < 1$,

$$\begin{aligned}\dot{X} &= -\frac{V_o}{L}(1-\delta) + \frac{V_{PV}(i_L)}{L} \\ &= -\frac{V_o}{L}(1-\delta_{eq} - k\sigma) + \frac{V_{PV}(i_L)}{L} \\ &= -\frac{V_o}{L}(1-(1-\frac{V_{PV}(i_L)}{V_o}) - k\sigma) + \frac{V_{PV}(i_L)}{L} \\ &= \frac{V_o}{L}k\sigma\end{aligned} \quad (23)$$

Based on the result of (22) and (23), $\dot{\sigma}$ always has inverse sign of σ. Therefore, $\dot{\sigma}\sigma < 0$ is obtained for $0 < \delta < 1$.

For $\delta = 1$,

$$\dot{X} = \frac{V_{PV}(i_L)}{L} > 0 \quad (24)$$

By (22) and (24), $\dot{\sigma} < 0$. With $\delta = 1$, two cases should be examined for the fulfillment of $\dot{\sigma}\sigma < 0$.

1) $\delta_{eq} = 1$

   If $\delta_{eq} = 1$, it implies $V_{\text{pv}}(i_L) = 0$ which means the system is operating at the left-hand corner of Fig. 5, and σ is negative for this case. Therefore, $\delta_{eq} + k\sigma$ will be less than 1, which contradicts to the assumption of $\delta = 1$.

2) $\delta_{eq} < 1$ and $\delta_{eq} + k\sigma \geq 1$

   If $\delta_{eq} < 1$, but $\delta_{eq} + k\sigma \geq 1$, it implies $\sigma > 0$ and $\dot{\sigma}\sigma < 0$.

It concludes that $\dot{\sigma}\sigma < 0$ for $\delta = 1$.

For $\delta = 0$,

$$\dot{X} = -\frac{V_o}{L} + \frac{V_{PV}(i_L)}{L} < 0 \quad (25)$$

In this case, the output voltage (V_o) is higher than the input voltage (V_{pv}). From (22) and (25), it results that $\dot{\sigma} > 0$. Two cases for $\delta = 0$ are examined as follows.

1) $\delta_{eq} = 0$

   $\delta_{eq} = 0$ implies $V_{PV}(i_L) = V_O$, which corresponding to the situation that the PV module is directly connected to the load and operates in the region $\sigma > 0$. As the result $\delta > 0$ and it contradicts to the assumption of $\delta = 0$.

2) $\delta_{eq} > 0$ and $\delta_{eq} + k\sigma \leq 0$

   In this case, $\sigma < 0$ is obtained and $\dot{\sigma}\sigma < 0$.

It concludes that $\dot{\sigma}\sigma < 0$ for $\delta = 0$.

From the discussion above, the existence of the MPP state $\sigma = 0$ can be guaranteed using the proposed control law (14). One thing worth to notice, to avoid the controller always saturates on the states $\delta = 0$ or $\delta = 1$ without hitting the range of $0 < \delta < 1$, the scaling constant k should not be selected to large (e.g. $k \leq 1/|\sigma|_{\max}$), where $|\sigma|_{\max}$ is the maximum absolute value of sliding surface $\sigma \cdot |\sigma|_{\max}$ presents when $\delta_{eq} = 0$,

$$\begin{aligned}|\sigma|_{\max} &= \sigma|_{\delta_{eq}=0} \\ &= -\frac{k_b TA}{q}\frac{I_0}{I_{ph} + I_0 + I_{PV}} + R_L \approx R_L\end{aligned} \quad (26)$$

Hence k□1/R_L can avoid the situation.

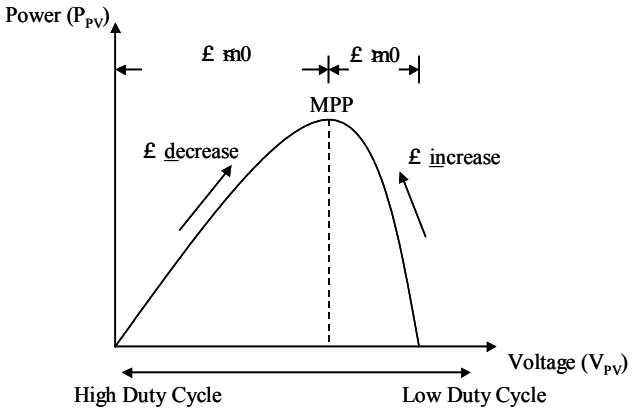

Fig. 5 Duty cycle versus operation region

5. Numerical Results

The PV model, boost type converter model, and proposed MPPT approach are implemented in Matlab / Simulink as illustrated in Fig. 6. In the study, KC-60 PV module manufactured by Kyocera Solar Inc. has been selected as PV power source, and the parameter of the components are chosen to deliver maximum 60W of power generated by KC-60. The specification of the system is tabulated in

table 1. The proposed MPPT is evaluated from three aspects: robustness to irradiance, temperature, and load. In each figures, two different values of irradiance, temperature or load are presented for comparison in order to show the robustness.

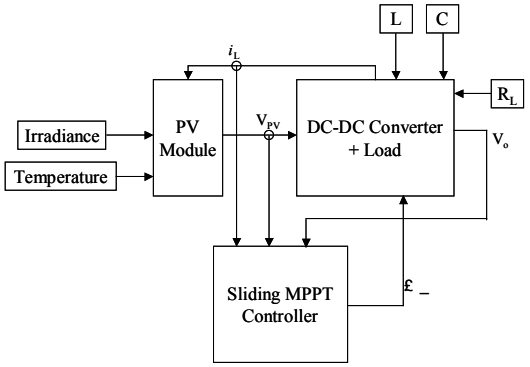

Fig. 6 MPPT system block diagram

Table 1 System specification

Parameters	Value	Parameters	Value
I_{rr}	5.981x10^{-8} (A)	q	1.6x10^{-19} (C)
I_{scr}	3.81 (A)	k_b	1.38x10^{-23} (J/K)
T_r	298 (K)	E_g	1.12 (V)
K_i	0.0024	A	1.2
L	1.5 (mH)	C	500 (uF)
k	0.001		

Fig. 7 illustrates the tracking result with step irradiance input (500 W/m^2 -> 1000W/m^2) under the same temperature and load. The system reaches steady state of both irradiance levels within the order of milliseconds, which is much faster compare to the other MPPT tracking techniques. Fig. 8 and 9 depict respectively the system response under rapid temperature change and load variation. In Fig. 8, sliding control MPPT is tested under sudden change of temperature from 273K to 323K, which is quite normal for space application. And Fig. 9 simulates the transit of a lightly loaded system to a heavily loaded system (From 100Ω to 10Ω). For all the results above, the sliding mode approach is able to maintain the output at optimum point and robust to the variation of the external conditions. Furthermore, it can almost reach the theoretical maximum power of known irradiance and temperature. The theoretical maximum powers of simulated condition are tabulated in Table 2.

6. Conclusion

In this paper, an approach for peak power tracking using the sliding mode control was proposed. The proposed controller is robust to environment changes and load variations. The stability and robustness of the controller were also validated. The performance of the controller was demonstrated through numerical studies.

Table 2 Theoretical maximum power

Irradiance (W/m^2)	Temperature (K)	Maximum power (W)
500	300	28.51
1000	300	59.78
1000	273	63.70
1000	323	55.71

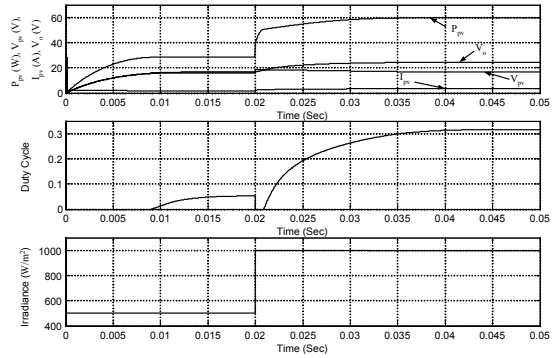

Fig. 7 Simulation with step irradiance change (500W/m^2 -> 1000W/m^2 , Temp = 300K, R_L= 10Ω)

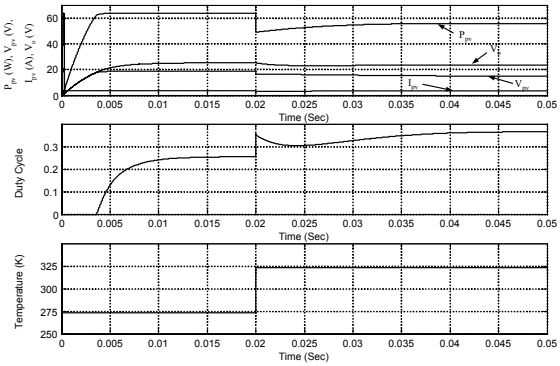

Fig. 8 Simulation with step temperature change (273K -> 323K , Irr = 1000W/m^2, R_L= 10Ω)

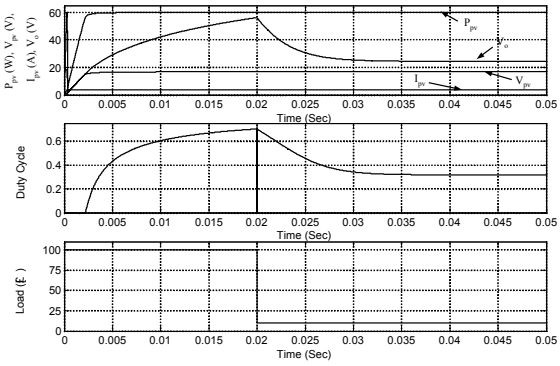

Fig. 9 Simulation with step load change (100Ω-> 10Ω, Irr = 1000W/m^2, Temp = 300K)

Acknowledgement

Part of this work was supported by the National Science Council, Taiwan, under the grant No. NSC94-2212-E006-020.

References

[1] W. Xiao, W.G. Dunford, "A modified adaptive hill climbing MPPT method for photovoltaic power systems," in 35th Annual IEEE Power Electronics. Specialists Conference, 2004, pp.1957-1963

[2] E. Koutroulis, K. Kalaitzakis, and N. C. Voulgaris, "Development of a microcontroller-based, photovoltaic maximum power point tracking control system", IEEE Trans. Power Electronics, vol.16, pp.46-54

[3] M. Veerachary, T. Senjyu, and K. Uezato, "Maximum power point tracking control of IDB converter supplied PV system", IEE Proc. Electronics Power Applications, 2001, pp.494-502

[4] C. Hua, J. Lin, "An on-line MPPT algorithm for rapidly changing illuminations of solar arrays", Renewable energy, Vol.28, Issue 7, pp.1129-1142

[5] N. Femia, G. Petrone, G. Spagnuolo, and M. Vitelli, "Optimization of Perturb and Observe Maximum Power Point Tracking Method", IEEE Trans. Power Electron., vol. 20, pp. 963-973

[6] Y.C. Kuo, T.J. Liang, and J.F. Chen, "Novel maximum-power-point tracking controller for photovoltaic energy conversion system", IEEE Trans. Ind. Electron., vol. 48, pp. 594-601

[7] K.H. Hussein, I. Mota, "Maximum photovoltaic power tracking: an algorithm for rapidly changing atmospheric conditions," in IEE Proc. Generation, Transmission, and Distribution, 1995, pp. 59-64.

[8] G.J. Yu, Y.S. Jung, J.Y. Choi, G.S. Kim, "A novel two-mode MPPT control algorithm based on comparative study of existing algorithms", Solar Energy, Vol.76, Issue 4, pp.455-463

[9] T. Noguchi, S. Togashi, R. Nakamoto, "Short-current pulse-based maximum-power-point tracking method formultiple photovoltaic-and-converter module system", Vol. 49, Issue 1, pp-217-223

[10] K. Kobayashi, H. Matsuo, and Y. Sekine, "A novel optimum operating point tracker of the solar cell power supply system," in 35th Annual IEEE Power Electronics Specialists Conference, 2004, pp. 2147-2151

[11] M. G. Simoes, N. N. Franceschetti, and M. Friedhofer, "A fuzzy logic based photovoltaic peak power tracking control," in Proc. 1998 IEEE International Symp. on Ind. Electron., 1998, pp. 300-305.

[12] B.M. Wilamowski, X. Li, "Fuzzy system based maximum power point tracking for PV system", IEEE 2002 28th Annual Conference of the industrial Electronics Society (IECON 02), 2002, pp.3280-3284

[13] T. Hiyama, S. Kouzuma, and T. Imakubo, "Identification of optimal operating point of PV modules using neural network for real time maximum power tracking control," IEEE Trans. Energy Conversion, vol.10, pp.360-367

[14] H. Tarik Duru, " A maximum power tracking algorithm based on Impp = f(Pmax) function for matching passive and active loads to a photovoltaic generator", Solar Energy, Vol.80, Issue 7, pp.812-822

[15] J-J E. Slotine, W. Li, "Applied Nonlinear Control", Prentice-Hall, 2005

[16] R.W. Erickson, D. Maksimovic, "Fundamentals of power electronics", Kluwer Academic Publishers, 2001

[17] H. De Battista, R.J. Mantz, "Variable structure control of a photovoltaic energy converter", IEE Proceedings- Control theory and applications, Vol.149, Issue 4, pp303-310

[18] I. Kim, "Sliding mode controller for the single-phase grid-connected photovoltaic system", Applied Energy, Vol.83, Issue 10, pp.1101-1115

[19] E. Fossas, D. Biel,"A Sliding Mode Approach to Robust Generation on dc-to-dc Nonlinear Converters", IEEE International Workshop on Variable Structure Systems, December 1996, pp.67-71

[20] S. Tan, Y.M. Lai, C.K.Tse, M.K.H. Cheung, "An adaptive sliding mode controller for buck converter in continuous conduction mode", Applied Power Electronics Conference and Exposition (APEC'04), 2004, pp.1395-1400.